MOLECULAR ONCOLOGY 10 (2016) 1232–1244

available at www.sciencedirect.com

ScienceDirect

www.elsevier.com/locate/molonc

A novel approach to detect resistance mechanisms reveals FGR as a factor mediating HDAC inhibitor SAHA resistance in B-cell lymphoma

Maria Joosten[a,1], Sebastian Ginzel[b,c,1], Christian Blex[d], Dmitri Schmidt[d], Michael Gombert[b], Cai Chen[b], René Martin Linka[b], Olivia Gräbner[d], Anika Hain[e], Burkhard Hirsch[a], Anke Sommerfeld[a], Anke Seegebarth[a], Uschi Gruber[d], Corinna Maneck[d], Langhui Zhang[b,f], Katharina Stenin[d], Henrik Dieks[d], Michael Sefkow[d], Carsten Münk[e], Claudia D. Baldus[g], Ralf Thiele[c], Arndt Borkhardt[b], Michael Hummel[a], Hubert Köster[d], Ute Fischer[b,2], Mathias Dreger[d,2], Volkhard Seitz[a,*,2]

[a]Institute of Pathology, Charité University Medicine, Campus Benjamin Franklin, Hindenburgdamm 30, 12200 Berlin, Germany

[b]Department of Pediatric Oncology, Hematology and Clinical Immunology, Center of Child and Adolescent Health, Medical Faculty, Heinrich-Heine-University, Moorenstr. 5, 40225 Düsseldorf, Germany

[c]Department of Computer Science, Bonn-Rhine-Sieg University of Applied Sciences, Grantham-Allee 20, 53757 Sankt Augustin, Germany

[d]caprotec bioanalytics GmbH, Magnusstraße 11, 12489 Berlin, Germany

[e]Clinic for Gastroenterology, Hepatology and Infectiology, Medical Faculty, Heinrich-Heine-University, Moorenstrasse 5, 40225 Düsseldorf, Germany

[f]Department of Hematology, Union Hospital, Fujian Medical University, NO.29,Xinquan Road, Fuzhou City, Fujian Province, China

[g]Department of Hematology and Oncology, Charité University Medicine, Campus Benjamin Franklin, Hindenburgdamm 30, 12200 Berlin, Germany

ARTICLE INFO

Article history:
Received 15 January 2016
Received in revised form
2 June 2016
Accepted 3 June 2016
Available online 9 June 2016

ABSTRACT

Histone deacetylase (HDAC) inhibitors such as suberoylanilide hydroxamic acid (SAHA) are not commonly used in clinical practice for treatment of B-cell lymphomas, although a subset of patients with refractory or relapsed B-cell lymphoma achieved partial or complete remissions.

Therefore, the purpose of this study was to identify molecular features that predict the response of B-cell lymphomas to SAHA treatment. We designed an integrative approach combining drug efficacy testing with exome and captured target analysis (DETECT). In this study, we tested SAHA sensitivity in 26 B-cell lymphoma cell lines and determined

Abbreviations: BL, Burkitt lymphoma; CC, capture compound; CCMS, capture compound mass spectrometry; CRISPR, Clustered Regularly Interspaced Short Palindromic Repeats; DETECT, drug efficacy testing combined with exome and captured target analysis; DLBCL, diffuse large B-cell lymphoma; FGR, Gardner-Rasheed feline sarcoma viral (v-fgr) oncogene homolog; HDAC, histone deacetylase; IC_{50}, half maximal inhibitory concentration; NHL, Non-Hodgkin lymphoma; SAHA, suberoylanilide hydroxamic acid.

* *Corresponding author.* Institute of Pathology, Charité University Medicine Berlin, Campus Benjamin Franklin, Hindenburgdamm 30, 12000 Berlin, Germany. Tel.: +49 30 84452734; fax: +49 30 4507536928.
E-mail address: volkhard.seitz@charite.de (V. Seitz).

[1] MJ and SG contributed equally to this work.
[2] UF, MD and VS contributed equally to this work.

http://dx.doi.org/10.1016/j.molonc.2016.06.001

Keywords:
SAHA
HDAC inhibitor
FGR
B-cell lymphoma
Drug resistance

SAHA-interacting proteins in SAHA resistant and sensitive cell lines employing a SAHA capture compound (CC) and mass spectrometry (CCMS). In addition, we performed exome mutation analysis. Candidate validation was done by expression analysis and knock-out experiments.

An integrated network analysis revealed that the Src tyrosine kinase Gardner-Rasheed feline sarcoma viral (v-fgr) oncogene homolog (FGR) is associated with SAHA resistance. FGR was specifically captured by the SAHA-CC in resistant cells. In line with this observation, we found that FGR expression was significantly higher in SAHA resistant cell lines. As functional proof, CRISPR/Cas9 mediated *FGR* knock-out in resistant cells increased SAHA sensitivity. *In silico* analysis of B-cell lymphoma samples (n = 1200) showed a wide range of FGR expression indicating that FGR expression might help to stratify patients, which clinically benefit from SAHA therapy.

In conclusion, our comprehensive analysis of SAHA-interacting proteins highlights FGR as a factor involved in SAHA resistance in B-cell lymphoma.

1. Introduction

During the past decades, epigenetics has emerged as an important area in drug discovery. So called “epidrugs” are defined as drugs that inhibit or activate disease-associated epigenetic proteins to ameliorate or cure the disease (Ivanov et al., 2014). Especially inhibitors of histone deacetylases (HDAC) are considered to be promising anticancer agents. By regulating acetylation states of histone and several non-histone proteins, they directly induce modifications in the cancer epigenome. Thereby, epigenetically silenced genes are re-expressed eventually resulting in growth arrest or apoptosis of cancer cells (Carew et al., 2008). Due to this anti-tumor activity, HDAC inhibitors had a rapid phase of clinical development as monotherapy and in combination with other anticancer drugs (Budde et al., 2013; Kirschbaum et al., 2011; Morschhauser et al., 2015; Ogura et al., 2014; Oki et al., 2013; Straus et al., 2015; Watanabe et al., 2010). However, a broad clinical response has been observed in patients with hematologic or solid malignancies ranging from complete remissions to no response (Chun, 2015).

Suberoylanilide hydroxamic acid (SAHA) (Vorinostat, Zolinza® (Merck and Co., Inc.)) was the first HDAC inhibitor approved by the American Food and Drug Administration in October 2006 for the treatment of a subset of patients with cutaneous T-cell lymphoma (Mann et al., 2007). Furthermore, SAHA is also used in clinical trials for patients with other types of Non-Hodgkin lymphoma (NHL) (Budde et al., 2013; Kirschbaum et al., 2011; Ogura et al., 2014; Straus et al., 2015; Watanabe et al., 2010).

NHL is a heterogeneous group of lymphoproliferative neoplasms. Two aggressive subtypes of B-cell NHLs are diffuse large B-cell lymphoma (DLBCL) and Burkitt lymphoma (BL), which account for 40% and 2% of all NHLs, respectively (Siegel et al., 2015; Swerdlow et al., 2008). Although survival of patients with B-cell lymphoma has improved by the addition of targeted therapies to conventional chemotherapy regimens, a considerable proportion relapse leading to adverse clinical outcome (Coiffier et al., 2010; Hoelzer et al., 2014; Reeder and Ansell, 2011; Sweetenham et al., 1996). Thus, novel approaches are urgently needed to improve disease control and patient’s survival. More specific and therefore less toxic treatment opportunities would be highly desirable (Chun, 2015). Preclinical and clinical studies with SAHA mono- or combination therapies showed promising results for the treatment of patients with B-cell lymphoma (Kirschbaum et al., 2011; Ogura et al., 2014; Richter-Larrea et al., 2010; Watanabe et al., 2010). Remarkably, response rates of up to 30% were achieved in patients with relapsed or refractory B-cell lymphoma upon SAHA monotherapy, comprising also complete remissions (Kirschbaum et al., 2011; Ogura et al., 2014; Watanabe et al., 2010). 70% of patients, however, do not respond to this treatment. Therefore, it is essential to identify those patients who will not benefit from HDAC inhibitor therapy in order to prevent ineffective treatment.

These clinical data stimulated us to seek for molecular features that help to stratify upfront B-cell lymphoma patients for SAHA treatment. To this end, we hypothesized (i) that proteins, which directly interact with SAHA, may be involved in SAHA response and (ii) that the expression and mutation status of these direct SAHA targets might be of relevance for SAHA response.

Direct SAHA interaction partners can be identified by Capture Compound Mass Spectrometry (CCMS). CCMS is based on a trifunctional small molecular probe called Capture Compounds (CC). SAHA is attached as selectivity function to a CC-scaffold that can interact with the target proteins in homogeneous phase under equilibrium conditions. The reactivity function of the CC-scaffold covalently binds the target proteins through photo-induced cross-linking. The sorting function of the CC-scaffold (e.g. biotin) enables the isolation of CC-proteins conjugates from complex protein mixtures (Supplemental Figures. S1 and S2). Finally, captured proteins are identified using high-resolution mass spectrometry (Fischer et al., 2011b; Koster et al., 2007).

To comprehensively identify the molecular mechanisms leading to SAHA resistance we designed an approach that applies **d**rug **e**fficacy **t**esting with **e**xome and **c**aptured **t**arget

analysis (DETECT; Figure 1). In detail, we combined (i) determination of SAHA sensitivity in 26 B-cell lymphoma cell lines by flow cytometry (Annexin V/propidium iodide staining) with (ii) analysis of exome mutations, (iii) CCMS of direct SAHA binders in SAHA resistant versus sensitive B-cell lymphoma cell lines and (iv) performed an integrated network analysis. For further candidate validation, we carried out expression analysis and knock-out experiments. To provide evidence for clinical relevance, *in silico* expression and mutation analysis of published data derived from B-cell lymphoma patients were performed.

Our DETECT approach led to the identification of SAHA-interacting protein networks and highlights the Src tyrosine kinase FGR as a factor mediating SAHA resistance in B-cell lymphoma.

2. Methods

2.1. Human cell lines and culture

26 human B-cell lymphoma cell lines (16 DLBCL and 10 BL cell lines) were used in this study, which were obtained from DSMZ or kindly provided by Georg Lenz. Details about cell lines and culture conditions are given in Supplemental Methods (section 1.1) and in Supplemental Table 1.

2.2. SAHA efficacy testing

26 B-cell lymphoma cell lines were seeded in triplicates into 12 well plates at a density of 3×10^5 cells per well and treated with either vehicle (DMSO) or varying concentrations (0.03 μM, 0.06 μM, 0.12 μM, 0.25 μM, 0.5 μM, 1 μM, 2 μM, 4 μM, 8 μM, 16 μM, 32 μM) of the HDAC inhibitor SAHA (Cayman Chemical) for 48 h.

Subsequently, apoptosis was determined by flow cytometry (Accuri C6; Becton, Dickinson and Company (BD)) using the APC Annexin V Apoptosis Detection Kit with propidium iodid (PI) (Biolegend) according to the manufacturer's instructions. Data were analyzed employing Accuri C6 software (BD). The inhibitory concentration IC_{50} was defined as the concentration of SAHA needed to decrease cell viability by 50%. Data were analyzed using Prism 6 (GraphPad Software, Inc.).

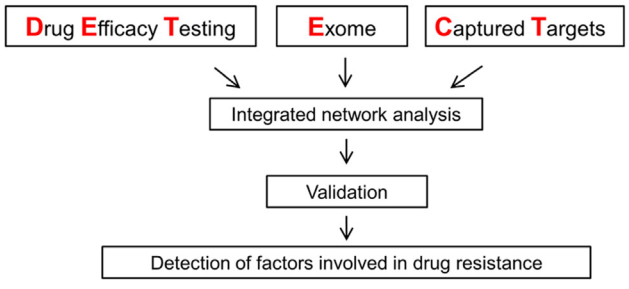

Figure 1 – DETECT workflow. In order to detect factors responsible for drug resistance, drug efficacy testing, exome mutation analysis and the determination of direct drug targets using CCMS are employed. An integrative network analysis of these data reveals potential candidates. Subsequently candidates are validated.

2.3. Cellular protein extraction and CCMS experiments

Cells were lysed in buffer containing 20 mM HEPES/NaOH pH 7.4, 250 mM sucrose, 5 mM $MgCl_2$, 1 mM DTT, 0.5% (w/v) n-dodecyl-β-maltoside supplemented with complete™ protease inhibitor cocktail (Roche) and benzonase using a glass–glass douncer. The extracts were cleared by centrifugation for 30 min at 100,000 × g. The protein content was determined using the bicinchoninic acid assay (BCA) method (Smith et al., 1985).

Synthesis and characterization of the SAHA-CC (Supplemental Figure S1) and CCMS experiments (Supplementary Figure S2) were performed as previously described (Fischer et al., 2011b).

Briefly, 114 μg of total protein was used for each sample. The SAHA-CC and free SAHA as competitor were employed at a final concentration of 10 μM and of 56 μM, respectively. Capture assays, competition control samples, and bead controls (without CC) were prepared in hexaplicate from four SAHA resistant and four SAHA sensitive cell lines.

Experimental conditions for CCMS were designed to identify both high and moderate affinity SAHA binding proteins. Buffer conditions were chosen that most likely native protein–protein interactions were preserved throughout all steps of the experiment. Under these conditions, primary SAHA binders can be specifically captured along with their protein–-protein interaction partners.

The captured proteins were proteolyzed and subjected to analysis by nanoflow liquid chromatography-tandem mass spectrometry (nLC-MS/MS). For the identification and quantification of protein intensities across the different samples from the different cell lines, the software package MaxQuant was used, applying the label-free quantification option (Cox and Mann, 2008). Further details on dose-dependent CCMS experiments, cross-competition studies, kinase assay, nLC-MS/MS, data acquisition and analysis are described in Supplemental Methods (sections 1.2–1.6).

2.4. Whole-exome sequencing, data analysis and validation

Whole-exome library preparation and sequencing of the 26 B-cell lymphoma cell lines was performed as described (Chen et al., 2013). Briefly, exome capture was carried out using the SeqCap EZ Exome Library 2.0 kit (Roche/Nimblegen) and 100 bp single-read sequencing was performed on a HiSeq2500 (Illumina). 82% of the coding region was covered at least 30×. Data were analyzed as previously reported and described in detail in the Supplemental Methods section 1.7 (Chen et al., 2013). Whole-exome sequencing data were deposited at the European Genome-phenome Archive (EGA, http://www.ebi.ac.uk/ega/), which is hosted by the EBI under the accession number EGAS00001001463. Randomly chosen nucleotide variations (n = 69) were validated by PCR and Sanger sequencing as described (Chen et al., 2013).

2.5. Integrated network analysis

To construct a protein–protein interaction network of all proteins detected in the SAHA capture experiments, we used

StringDB (Franceschini et al., 2013). Medium confidence interactions (>0.4) were taken into account, if they were not solely based on text mining methods.

To incorporate the exome data, we considered a ranking of possible effects of mutations as defined by the Ensembl analysis group (Supplemental Table S2) and determined which gene carries more detrimental mutations in SAHA resistant compared to SAHA sensitive cells (Flicek et al., 2014; McLaren et al., 2010). Only mutations with a frequency of less than 15% in the 1000 genomes project were considered to remove common variations. Different attributes from CC-enrichment and whole exome analysis were mapped to the graph and visualized using Cytoscape (Shannon et al., 2003).

2.6. Protein extraction and Western blot analyses

Protein extraction and Western blot analysis were performed as described previously (Dimitrova et al., 2014). The primary antibodies used for Western blot analysis were anti-FGR (clone 1B12; Abnova) and anti-beta actin (AC-15; Abcam). The secondary goat anti-mouse IgG/HRP antibody was purchased from Dako (P0447) and the donkey anti-rabbit IgG/HRP antibody from GE Healthcare Life Sciences (NA9340). Western blot bands were quantified with the FusionCapt Advance software (Vilber Lourmat).

2.7. RNA isolation, cDNA synthesis and real-time reverse transcriptase (RT) polymerase chain reaction (PCR)

RNA was isolated and cDNA synthesized as described previously (Joosten et al., 2013). Real-time RT PCR was performed with SYBR Green PCR-Master Mix (Applied Biosystems) by a StepOnePlus real-time PCR system (Applied Biosystems) using the PCR parameters recommended by the manufacturer. The housekeeping gene *GAPDH* was amplified in parallel with *FGR* (FGR: forward: 5′-GGCCCGGCCTGCAT-3′; reverse: 5′-TTGATGGCCTGAGAGGAGAAG-3′; GAPDH: forward: 5′-AGGTGGAGGAGTGGGTGTCGCTGTT-3′; reverse: 5′-CCGGGAAACTGTGGCGTGATGG-3′). Primers were purchased from Eurofins MWG. Relative mRNA quantification was calculated using the comparative $\Delta\Delta C_T$ method (Bookout and Mangelsdorf, 2003). A two-sided Mann Whitney U test was employed to test significant differences in *FGR* expression between SAHA resistant and sensitive cell lines.

2.8. FGR knock-out by CRISPR/Cas9

Knock-out of the *FGR* gene was done by CRISPR/Cas9 mediated double strand breaks leading to insertions/deletions after repair via the non-homologous end-joining pathway (Cong et al., 2013; Mali et al., 2013). The heterogeneous genotype of the *FGR* locus in the resulting cell populations was analyzed by amplicon sequencing. Methodical details are provided in Supplemental Methods (section 1.8).

2.9. In silico *FGR* expression and mutation analysis in B-cell lymphoma patients

For the analysis of publicly available gene expression data sets of B-cell lymphoma samples (n = 1200) the R2 application was used (R2: Genomics Analysis and Visualization Platform (http://r2.amc.nl)) (Dave et al., 2006; Hummel et al., 2006; Richter et al., 2012; Scholtysik et al., 2015; Visco et al., 2012). For compilation of published tumor associated somatic nucleotide variations in B-cell lymphoma samples (n = 413) the cosmic database (v74) was employed (Forbes et al., 2015).

3. Results

3.1. Determination of SAHA resistant and sensitive B-cell lymphoma cell lines

26 B-cell lymphoma cell lines were treated with increasing concentrations of SAHA for 48 h. Cell lines with IC50 values ≥2.5 μM SAHA were classified as resistant and cell lines with IC50 values ≤2.0 μM SAHA as sensitive. Cell lines with IC50 values between 2.0 and 2.5 μM were classified as intermediate. Classification was based on the average plasma concentration of SAHA in patients (2.5 μM) (Iwamoto et al., 2013). According to these categories, we identified 11 SAHA resistant, 3 intermediate and 12 SAHA sensitive B-cell lymphoma cell lines (Table 1). The IC_{50} of the most resistant cell line (CA-46; IC_{50}: 470.4 μM SAHA) differed from the IC_{50} of the most sensitive cell line (OCI-Ly1; IC_{50}: 0.5 μM SAHA) by three orders of magnitude.

Table 1 – Categorization of 26 B-cell lymphoma cell lines in resistant, intermediate and sensitive based on their SAHA IC50 values. IC50 values were calculated using Prism6 (GraphPad Software, Inc.).

SAHA	Cell line	IC50 (μM SAHA)
Resistant	CA-46*	470.40
	Daudi*	282.60
	DG-75*	117.70
	Raji*	19.74
	Blue-1	11.72
	Namalwa	7.00
	DND-39	5.76
	HT	4.63
	BL-70	3.93
	Carnaval	3.56
	WSU-DLCL2	3.52
Intermediate	Kis-1	2.49
	SU-DHL-4	2.27
	OCI-Ly7	2.15
Sensitive	OCI-Ly2	1.98
	WSU-FSCCL	1.82
	HBL-1	1.62
	U2932	1.61
	SU-DHL-6	1.48
	Granta-452*	1.28
	BL-2	1.18
	OCI-Ly3	1.14
	BL-41*	1.13
	TMD8*	0.96
	OCI-Ly10	0.61
	OCI-Ly1*	0.50

*cell lines used for CCMS analysis.

3.2. *CCMS based SAHA interaction profiles in SAHA resistant and SAHA sensitive cell lines*

Following the hypothesis that alterations in the capture profiles of proteins or protein complexes interacting with SAHA contribute to the differential SAHA response of the cells, we profiled the four most SAHA resistant and four of the most SAHA sensitive cells lines for SAHA-binding proteins by CCMS.

We compiled a list of 315 candidate proteins that directly or indirectly interact with SAHA. This list contained previously described *bona fide* targets of SAHA (HDAC1, 2, 3, 6, 8, members of the HDAC1/2 complexes, ISOC1 and ISOC2) and a large number of novel proteins with unknown relation to HDACs (Supplementary Table S3A) (Bantscheff et al., 2011; Fischer et al., 2011b). Out of the 315 proteins compiled in our initial list, 129 were either predominantly enriched from SAHA

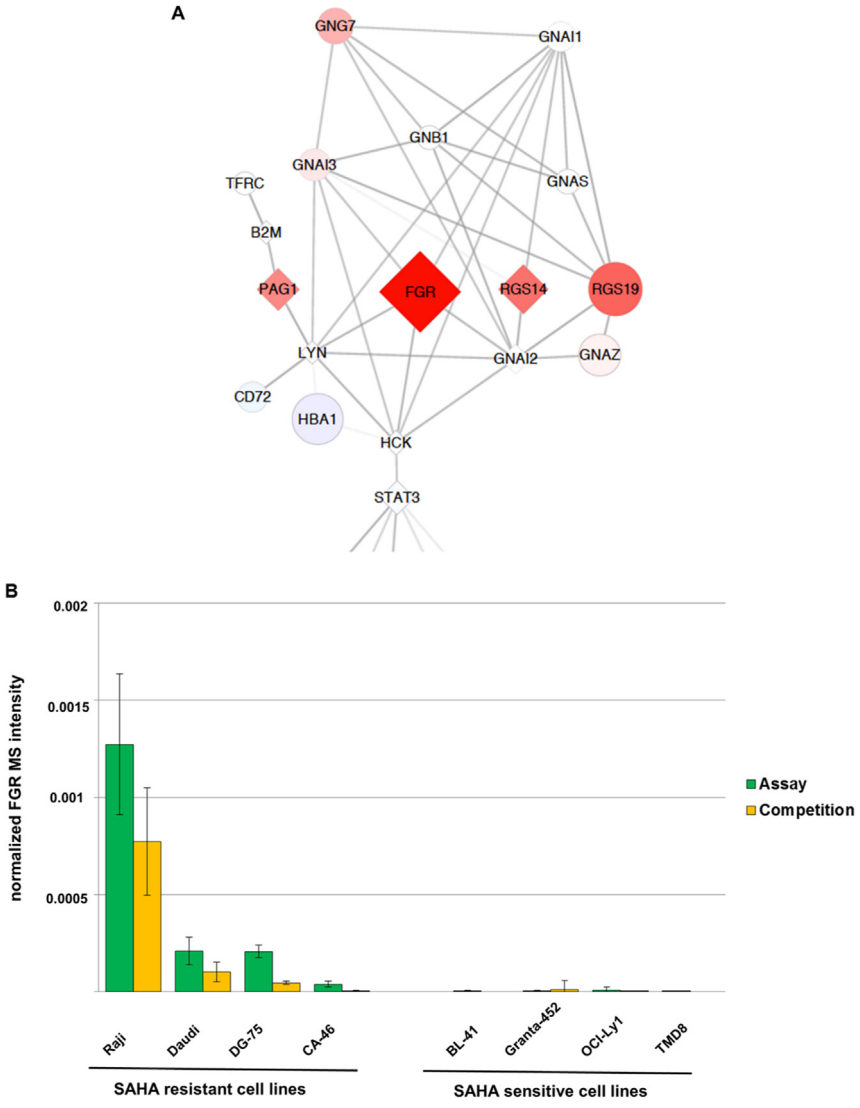

Figure 2 – FGR is a candidate for SAHA resistance in B-cell lymphoma. A: Within the integrated network of captured proteins and whole exome sequencing data the node color and size indicate fold changes towards SAHA resistant (red) or sensitive (blue) cell lines in the CCMS experiments, white nodes indicate no relevant fold change (logFC < 1), the transparency expresses the p-value. Diamond shaped nodes mark gene products that carry a more detrimental mutation as defined by the Ensembl analysis group in any of the SAHA resistant cell lines (Flicek et al., 2014). Edge opaqueness expresses protein interaction confidence. FGR showed significantly higher binding in all resistant cell lines during protein capture and carried more detrimental mutations in some resistant cell lines (3/11). Data were visualized using Cytoscape. The full graph is available as Supplemental Figure S3. B: Normalized mass spectrometric protein intensities for FGR across SAHA CCMS assay with and without SAHA competition across four SAHA resistant and four sensitive cell lines. The higher FGR enrichment by the SAHA-CC in resistant cell lines compared to sensitive cell lines was significant ($p = 9.6 \times 10^{-7}$). Regarding SAHA resistant cell lines, FGR enrichment was significantly higher in the SAHA CCMS assay with competitor as compared to SAHA capture assay without competitor ($^{*}p < 0.05$; $^{**}p < 0.001$). Assay: SAHA CCMS assay without competitor, Competition: SAHA CCMS in the presence of a 5.6-fold excess of unmodified SAHA as competitor. FGR protein intensities were determined by nLC-MS/MS followed by label-free quantification and data normalization.

resistant (n = 117) or from SAHA sensitive (n = 12) cell lines (Supplemental Table S3B).

3.3. Integrated network analysis reveals FGR as a candidate involved in SAHA resistance

To assess the functional context of significant SAHA binders, we generated a protein–protein interaction network from the 315 candidate proteins, which yielded 125 proteins that interact with each other (Supplemental Figure S3). Interestingly, in the largest connected subnetwork, a membrane associated and cytoplasmic network comprising mainly Src kinases (FGR, HCK, LYN), G-proteins and their regulators (GNAI1, GNAI2, GNAI3, GNG7, GNAZ, GNAS, GNB1, RGS14 and RGS19) was linked to nucleus-associated HDAC-complexes through the STAT-pathway (Figure 2A, Supplemental Figure S3). The integration of our exome data into this network revealed three proteins (FGR, RGS14, and PAG1), which carry more detrimental mutations according to the Ensembl analysis group in a small number of resistant cell lines (FGR: 3/11; RGS14: 2/11, PAG1: 1/11) (Figure 2A; Supplemental Figure S3; Supplemental Tables S4 and S5) (Flicek et al., 2014; McLaren et al., 2010). Among these proteins, FGR showed the highest and most significant ($p = 9.6 \times 10^{-7}$) CCMS enrichment in resistant cells compared to sensitive cells (Figure 2B; Supplemental Table S3). Taken together, our integrated network analysis identified networks of resistance mechanisms rather than single recurrent mutation. The highly significant CCMS intensity profile of FGR in all resistant cell lines prompted us to investigate the role of FGR in SAHA resistance.

3.4. Characterization of the SAHA-FGR interaction

To the best of our knowledge, FGR has never been reported before to interact with SAHA. Therefore, we characterized SAHA binding to FGR in more detail.

First, we determined FGR binding strength to SAHA. To this end, a series of CCMS experiments with Raji cell lysate were performed, at which the protein input was constant, but the SAHA-CC concentration varied from 0 to 10 μM across 14 different concentrations. The normalized mass spectrometric intensities of each individual protein across capture assays at the different concentrations of SAHA-CC determined by nLC-MS/MS yielded protein intensity profiles for each protein. The analysis of these intensity profiles revealed two clusters of proteins with (i) high (half-maximal capturing between 250 and 500 nM SAHA-CC) and (ii) moderate affinity (half-maximal capturing between 1 and 10 μM SAHA-CC). The high affinity cluster contained 24 proteins including several HDACs (e.g. HDAC1 and HDAC6) and HDAC protein interaction partners (Supplemental Figure S4). FGR was assigned to the moderate affinity cluster containing 78 proteins (Supplemental Figure S5). For FGR, half-maximal capturing occurred at a CC-concentration of ~2.5 μM compared to HDAC1 and HDAC6 with ~350 nM, and ~500 nM, respectively (Figure 3A). To estimate the apparent binding strength of SAHA to FGR, we determined the SAHA concentration

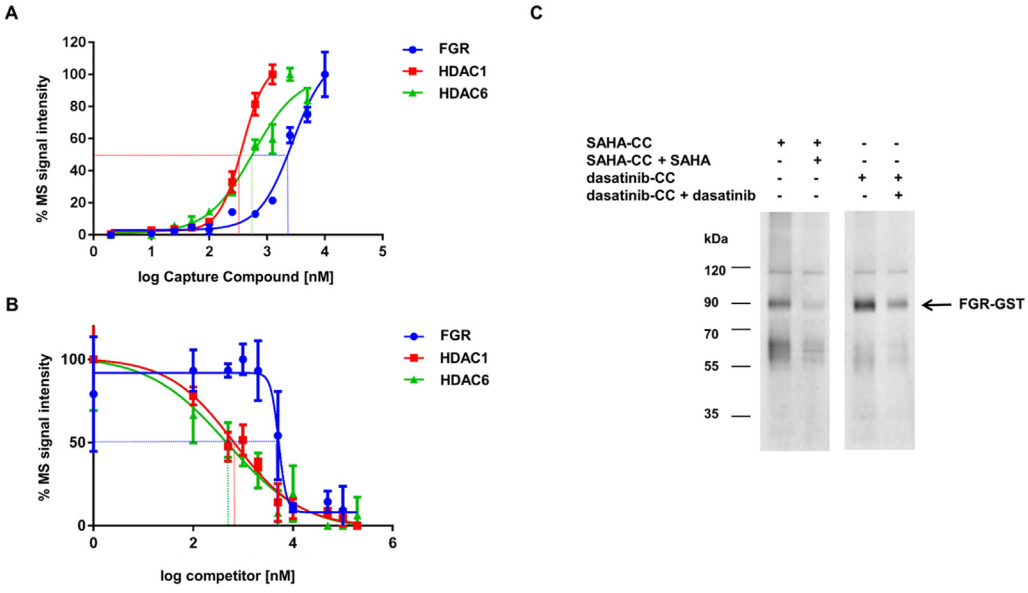

Figure 3 – Characterization of the SAHA-FGR interaction. A: Binding of the SAHA-CC to FGR based on CCMS titration experiment with Raji protein lysate. Half-maximal capturing of FGR by the SAHA-CC occurred at FGR = ~2.5 μM, HDAC1 ~ 375 nM, HDAC6 ~ 500 nM. B: Dose-dependent competition of FGR with SAHA based on CCMS competition titration experiment at a fixed CC-concentration of 2.5 μM with Raji protein lysate. Half-maximal competition occurred at FGR = 5.10 μM, HDAC1 = 970 nM, HDAC6 = 1.40 μM. The results of A and B suggest that SAHA binds to FGR with moderate affinity. C: Streptavidin-horseradish peroxidase Western blot showing specific biotinylation of recombinant FGR (FGR-GST) by the SAHA-CC and dasatinib-CC (positive control). The specific biotinylation by the SAHA-CC (final concentration 6.25 μM), which was abolished by the competitor (SAHA, final concentration 100 μM), indicates direct binding of SAHA to FGR. In the reference experiment, the dasatinib-CC was used at 1.25 μM, and dasatinib (competitor) at 100 μM. Western blots were documented using a G:BOX F3 Fluorescence Imaging System (Syngene).

required for half-maximal competition of the SAHA-CC-binding at a fixed SAHA-CC concentration of 2.5 μM. Half-maximal competition of the SAHA-CC binding to FGR occurred at a SAHA concentration of 5.1 μM compared to HDAC1 and HDAC6 with 0.97 μM, and 1.4 μM respectively (Figure 3B). These data confirmed that FGR is a SAHA binder with moderate affinity.

To prove direct binding of SAHA to FGR, we carried out CCMS experiments with purified human recombinant FGR. The SAHA-CC comprised a photo-inducible cross-linking and a biotin-sorting functionality. In case of direct SAHA binding, FGR should become biotinylated upon UV-induced cross-linking of the SAHA-CC. This biotinylation should be abolished in the presence of an excess of SAHA as competitor. As positive control and competitor, we used a dasatinib-CC and dasatinib respectively, since dasatinib is a known FGR inhibitor, which directly binds FGR with high affinity (Fischer et al., 2011a; Karaman et al., 2008). Employing Western blot analysis, we showed direct cross-linking of SAHA-CC to FGR, which was abolished in the presence of SAHA comparable to the positive dasatinib control (Figure 3C). Thus, SAHA binds directly to FGR.

To test whether SAHA is capable of inhibiting FGR kinase activity, we performed an FGR kinase activity inhibition assay comparing dasatinib with SAHA. While dasatinib inhibited FGR kinase activity in a low nM-range, SAHA was not able to inhibit FGR kinase activity even at the highest concentration tested (10 μM; data not shown). Accordingly, direct binding of SAHA to FGR can only be explained by a direct binding of SAHA to FGR via a binding site different from dasatinib. To this end, we tested whether the FGR binding sites for SAHA and dasatinib differ from each other. We conducted CCMS experiments using the SAHA-CC and performed competition experiments with either SAHA or dasatinib employing a CA-46 cell lysate. While SAHA largely abolished capturing of FGR by the SAHA-CC, capturing of FGR was only negligibly affected by dasatinib (Supplemental Figure S6). The data further support that SAHA binds FGR directly and specifically, but that the SAHA binding site is different from the dasatinib binding site.

3.5. *FGR expression status distinguished SAHA resistant from SAHA sensitive cell lines*

Since FGR showed the highest and most significant CC-enrichment in resistant cells compared to sensitive cells, we analyzed FGR RNA/protein expression in our B-cell lymphoma cell line panel (n = 26). FGR protein expression was clearly higher in SAHA resistant cell lines compared to SAHA sensitive cell lines (Figure 4A, Supplemental Table S6). In line with this, *FGR* RNA expression analysis in both groups revealed that the difference in *FGR* expression between resistant and sensitive cell lines was significant ($p = 1.0 \times 10^{-6}$) (Figure 4B). Thus, FGR expression is a strong indicator for SAHA resistance.

3.6. *FGR knock-out leads to increased SAHA sensitivity in FGR non-mutated cell lines*

To functionally validate the relation between FGR expression and SAHA resistance, three SAHA resistant cell lines (Daudi, Raji and DG-75) were chosen to knock-out *FGR* via CRISPR/Cas9 targeting. While Daudi and Raji have a non-mutated *FGR* gene, DG-75 harbors a heterozygous *FGR* mutation in its tyrosine kinase domain (c.1459/C>A). The resulting cell populations were composed of a heterogeneous genotype at the targeted locus with efficient *FGR* knock-out in Daudi (91% INDELs), and DG-75 (84.9% INDELs), while Raji only showed 51.8% INDELs (Figure 5A; Supplemental Table S7).

All cell lines were treated with different concentrations of SAHA (0–32 μM) to determine IC_{50} values. The lack of FGR clearly increased the sensitivity of Raji and Daudi to SAHA compared to control cells (Raji: 19.5 μM → 6.0 μM; Daudi: 287.2 μM → 55.9 μM; Figure 5B). Interestingly, the *FGR* mutated DG-75 cells showed no increase in SAHA sensitivity (117.5 μM → 132.5 μM; Figure 5B).

3.7. *FGR expression and mutation status in B-cell lymphoma patient samples*

The expression of *FGR in silico* was analyzed in publicly available datasets of 1200 B-cell lymphoma patients using the R2 application (Figure 4C) (Hummel et al., 2006; Richter et al., 2012; Scholtysik et al., 2015; Visco et al., 2012). The expression of *FGR* in B-cell lymphoma samples was distributed over a wide log range within the analyzed cohorts. This indicates that differences in FGR expression could potentially be used for a stratification of B-cell lymphoma patients prior to SAHA treatment.

We also analyzed publicly available sequencing data from 413 B-cell lymphoma patient samples (Forbes et al., 2015). Only one of the samples harbored a mutation in *FGR*, which indicates that *FGR* mutations are very rare in primary B-cell lymphoma.

4. Discussion

The HDAC inhibitor SAHA showed encouraging clinical response rates in patients with refractory or relapsed B-cell lymphoma after SAHA monotherapy (Kirschbaum et al., 2011; Ogura et al., 2014; Watanabe et al., 2010). Unfortunately, the majority of patients do not respond to this type of therapy posing the question for the underlying mechanisms. Therefore, the understanding of these molecular resistance mechanisms could pave the way to stratify patients that benefit from a HDAC inhibitor therapy and thus improve the efficacy of these promising drugs.

We hypothesized that the therapeutic effect of a drug is mainly based on the expression and mutation status of drug target proteins. To this end, we designed a novel approach combining **d**rug **e**fficacy **t**esting with whole-**e**xome data and **c**aptured **t**arget analysis (DETECT) to identify factors involved in drug resistance (Figure 1).

Here, we used DETECT to unravel SAHA resistance mechanisms in a panel of 26 B-cell lymphoma cell lines as a model system for the molecular mechanisms in B-cell lymphoma. While several studies have investigated mechanisms of HDAC resistance, so far direct binding proteins of SAHA were not examined in this context (Fantin et al., 2008; Fiskus et al., 2008; Garcia-Manero et al., 2008; Ierano et al., 2013;

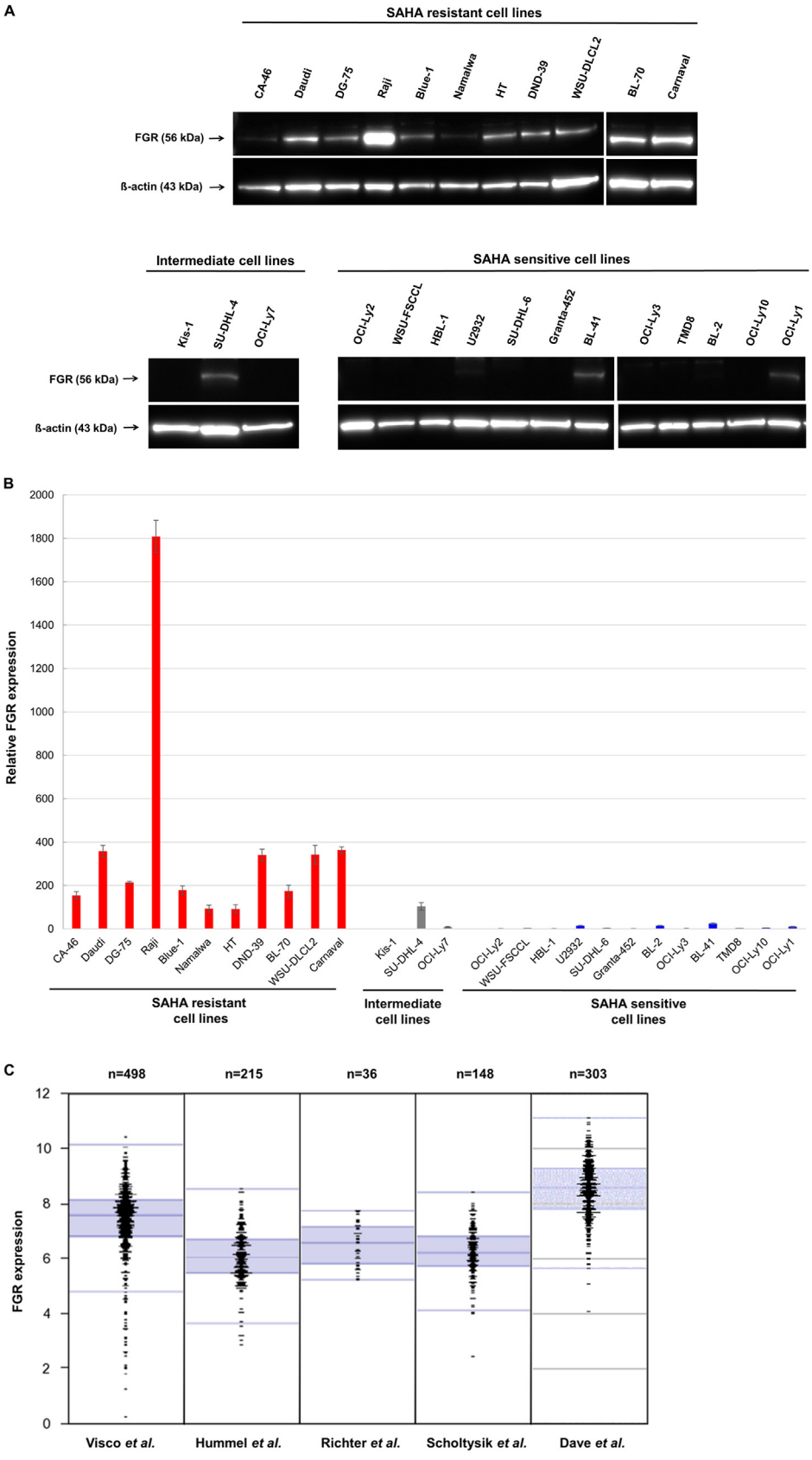

Figure 4 – FGR expression. A: Western blot analysis of B-cell lymphoma cell lines (n = 26) revealed that FGR expression is higher in SAHA resistant cell lines compared to intermediate and sensitive cell lines. β-actin was used as a loading control. Fusion software (Peqlab Biotechnologie GmbH) was employed to analyze Western blot bands. Narrow gaps indicate separately performed blots. B: Real-time RT-PCR analysis of B-cell lymphoma cell lines (n = 26) showed a higher expression of FGR in SAHA resistant cell lines compared to intermediate and sensitive cell lines.

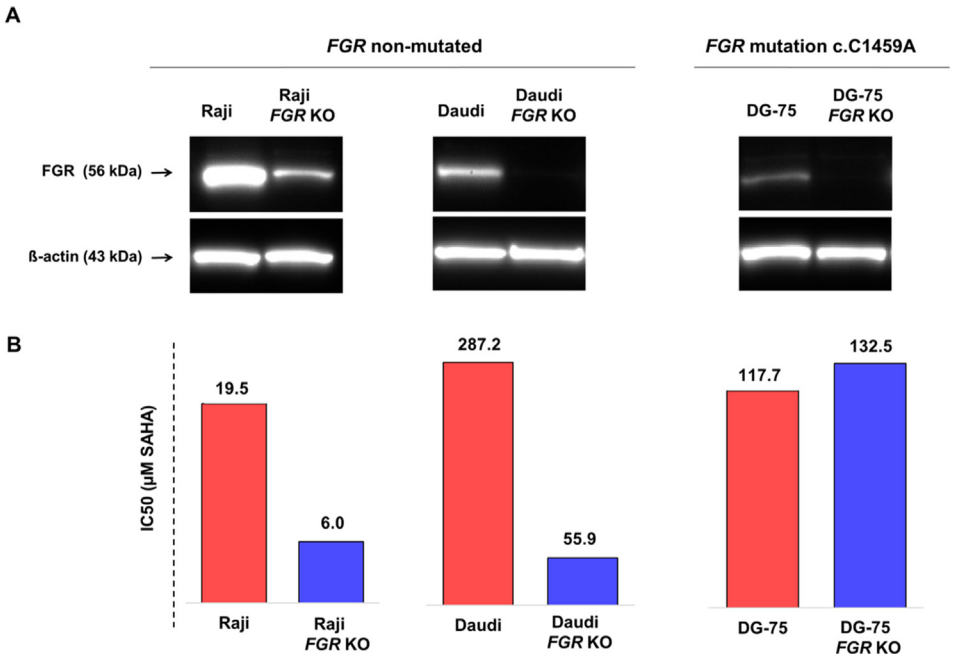

Figure 5 – Functional validation of FGR involvement in SAHA resistance. A: *FGR* knock-out (KO) in Raji, Daudi and DG-75 was confirmed by Western blot analysis. Compared to control (untransfected) cells, all three *FGR* knock-out cell lines showed an efficient knock-out of *FGR*. β-actin was used as a loading control. Fusion software (Peqlab Biotechnologie GmbH) was used to analyze Western blot bands. B: SAHA IC50 values for control and *FGR* knock-out cell lines were determined. Raji and Daudi (non-mutated *FGR*) showed an increase in SAHA sensitivity after *FGR* knock-out, whereas DG-75 (*FGR* mutation c.C1459A) had no change in SAHA sensitivity after *FGR* knock-out. IC50 values were calculated using Prism6 (GraphPad Software, Inc.).

Khan et al., 2010; Kim et al., 2015; Lee et al., 2011; Munster et al., 2009; Thompson et al., 2013). Furthermore, previous studies analyzing direct SAHA binding proteins did not focus on SAHA resistance mechanisms (Bantscheff et al., 2011; Fischer et al., 2011b; Salisbury and Cravatt, 2007).

Our SAHA sensitivity testing of B-cell lymphoma cell lines led to the identification of 11 SAHA resistant and 12 SAHA sensitive cell lines. Both, BL and DLBCL cell lines were present in SAHA sensitive and resistant groups. However, the BL cell lines showed the higher IC_{50} values (Table 1). Overall, the observation of resistant and sensitive cell lines nicely reflects the occurrence of responding and non-responding B-cell lymphoma patients.

SAHA CCMS data of four SAHA resistant and four SAHA sensitive cell lines led to the identification of 315 SAHA binding proteins. Combining the CCMS data with whole exome data of all 26 cell lines revealed a membrane associated and cytoplasmic subnetwork, comprising mainly membrane-associated Src kinases (FGR, HCK LYN) and G-proteins, linked to nucleus-associated HDAC-complexes through the STAT-pathway (Figure 2A and Supplemental Figure S3). Remarkably, mutations in FGR and its interaction partner RGS14 occurred in the same SAHA resistant cell lines (DG-75, HT) (Supplemental Table S4). Although multiple resistance factors are most likely involved in this SAHA relevant network, we focused on the role of FGR in SAHA resistance since it showed the highest and most significant CCMS enrichment.

First, we provided evidence of direct binding of SAHA to FGR and showed that the SAHA binding site for FGR must be different to the binding site of the FGR inhibitor dasatinib, which binds to the catalytic pocket. However, the exact site of SAHA binding to FGR remains unclear (Figure 3).

Next, we analyzed FGR expression in the 26 B-cell lymphoma cell lines (Figure 4 A/B; Supplemental Table S6). In line with our CCMS data, SAHA resistant cell lines showed a higher FGR expression and the difference in FGR expression between resistant and sensitive cell lines was significant for RNA and protein expression with p-values of 1.0×10^{-6} and

GAPDH was used for normalization. Note: Carnaval and Kis-1 showed increased CT values for GAPDH, which distort the quantitative FGR expression. Thus, the average CT value for GAPDH (19.9) was used to normalize Carnaval and Kis-1. Relative mRNA quantification was calculated using the comparative ΔΔCT method (Bookout and Mangelsdorf, 2003). Two-sided Mann-Whitney-U test revealed a significantly different FGR expression ($p = 1.035 \times 10^{-6}$) in SAHA resistant cell lines compared to sensitive cell lines. C: FGR expression is high and distributed over a wide range of B-cell lymphoma (n = 1200). Dot-boxplots present the $\log_2$ transformed FGR expression values of B-cell lymphoma patients recruited in five independent cohorts. Numbers of recruited patients are indicated. Gene expression was determined using an Affymetrix U133P2 chip and MAS5 normalization (Hummel et al., 2006; Richter et al., 2012; Scholtysik et al., 2015; Visco et al., 2012). In the Dave cohort, gene expression was analyzed using a custom oligonucleotide microarray with 2524 unique genes that are expressed differentially among a variety of non-Hodgkin lymphoma and MAS5 normalization (Dave et al., 2006). Plots were generated using R2.

6.0×10^{-5} respectively. However, FGR expression does not directly correlate with SAHA resistance, which might reflect the presence of multiple resistance factors.

To further prove the relation between FGR expression and SAHA resistance, we showed that FGR knock-out in SAHA resistant cell lines with high FGR expression led to increased SAHA sensitivity in non-mutated *FGR* cell lines. It is of note, that SAHA sensitivity was not increased by *FGR* knock-out in DG-75 carrying the heterozygous mutation in the kinase domain of *FGR* (Supplemental Figure S7). We speculate that DG-75 acquired mechanisms to circumvent a possible altered FGR function (Figure 5).

In the context of B-cell lymphoma, the direct interaction of SAHA with FGR is of special interest. FGR is clearly higher expressed in B-cell lymphoma cell lines compared to cell lines derived from non-lymphoid cancer entities (Supplemental Figure S8). Furthermore, FGR is a member of Src-family kinases (SFKs) – a group of membrane-associated non-receptor tyrosine kinases – which are key mediators in the B-cell receptor signaling (BCR) transduction cascade (Saijo et al., 2003). Other members of the SFKs are c-SRC, YES, FYN, LYN, LCK, HCK, BLK and YRK. Interestingly, HCK and LYN were also present in our network of SAHA interacting proteins (Figure 2A). Activated Src kinases phosphorylate cytoplasmic domains of BCR components that finally lead to the activation of transcription factors such as nuclear factor-κB, nuclear factor of activated T-cells (NFAT) and signal transducers and activators of transcription (STATs) (Dal Porto et al., 2004). Fantin et al. showed that SAHA resistant lymphoma cell lines (including B- and T-cell lymphoma) had higher expression levels of activated (phosphorylated) STAT1, STAT3 and STAT5 (Fantin et al., 2008). Interestingly, FGR is involved in phosphorylation of STATs (Schreiner et al., 2002). Moreover, our network analysis points towards a possible role of G-protein signaling being relevant for SAHA resistance mechanisms (Figure 2A).

Since we focused on FGR, we further tested the feasibility using FGR analysis to stratify B-cell lymphoma patients. For this purpose, we analyzed FGR expression and mutation status *in silico* by using publicly available data sets. *FGR* expression analysis in 1200 B-cell lymphoma patients revealed a wide range of *FGR* expression (Figure 4C). *FGR* mutations were a rare event in B-cell lymphoma patients (n = 1/413). Therefore, FGR mutations seem to be negligible and FGR expression is a promising parameter to stratify patients that might benefit from SAHA therapy.

In conclusion, the novel DETECT approach is a comprehensive strategy to gain a better understanding of drug resistance mechanisms. In this study, we describe a complex SAHA protein interaction network and identified FGR as a direct SAHA target protein being involved in SAHA resistance in B-cell lymphoma. FGR expression might be helpful to stratify patients, who have a clinical benefit from SAHA treatment.

Acknowledgements

We thank Hans-Henning Müller and Katayoun Alemazkour for excellent technical support, Georg Lenz for providing cell lines and Lora Dimitrova, Karsten Kleo, Dido Lenze, Marc Remke and Sefer Elezkurtaj for valuable discussion.

This work was supported by a grant from the "Zentrales Innovationsprojekt Mittelstand" (KF2766404CS2; KF2077503CS2; KF2986901CS2).

Appendix A. Supplementary data

Supplementary data related to this article can be found at http://dx.doi.org/10.1016/j.molonc.2016.06.001.

Authorship contributions

MJ, SG, CM, CDB, RT, AB, MH, HK, UF, MD and VS designed research. MJ, CB, DS, MG, CC, RML, OG, AH, ASo, ASe, UG, CM, LZ, KS, HD, MS performed experiments. MJ, SG, CB, DS, MG, CC, RML, OG, AH, BH, ASo, ASe, UG, CMü, AB, MH, HK, UF, MD, VS analyzed and interpreted data. MJ, SG, CM, CDB, RT, AB, MH, HK, UF, MD and VS wrote the manuscript. All authors reviewed and accepted the final version of the manuscript.

Disclosure of conflicts of interest

All authors have no conflict of interest to disclose.

REFERENCES

Bantscheff, M., Hopf, C., Savitski, M.M., Dittmann, A., Grandi, P., Michon, A.M., Schlegl, J., Abraham, Y., Becher, I., Bergamini, G., Boesche, M., Delling, M., Dumpelfeld, B., Eberhard, D., Huthmacher, C., Mathieson, T., Poeckel, D., Reader, V., Strunk, K., Sweetman, G., Kruse, U., Neubauer, G., Ramsden, N.G., Drewes, G., 2011. Chemoproteomics profiling of HDAC inhibitors reveals selective targeting of HDAC complexes. Nat. Biotechnol. 29, 255–265.

Bookout, A.L., Mangelsdorf, D.J., 2003. Quantitative real-time PCR protocol for analysis of nuclear receptor signaling pathways. Nucl. Recept Signal 1, e012.

Budde, L.E., Zhang, M.M., Shustov, A.R., Pagel, J.M., Gooley, T.A., Oliveira, G.R., Chen, T.L., Knudsen, N.L., Roden, J.E., Kammerer, B.E., Frayo, S.L., Warr, T.A., Boyd, T.E., Press, O.W., Gopal, A.K., 2013. A phase I study of pulse high-dose vorinostat (V) plus rituximab (R), ifosphamide, carboplatin, and etoposide (ICE) in patients with relapsed lymphoma. Br. J. Haematol. 161, 183–191.

Carew, J.S., Giles, F.J., Nawrocki, S.T., 2008. Histone deacetylase inhibitors: mechanisms of cell death and promise in combination cancer therapy. Cancer Lett. 269, 7–17.

Chen, C., Bartenhagen, C., Gombert, M., Okpanyi, V., Binder, V., Rottgers, S., Bradtke, J., Teigler-Schlegel, A., Harbott, J., Ginzel, S., Thiele, R., Fischer, U., Dugas, M., Hu, J., Borkhardt, A., 2013. Next-generation-sequencing-based risk stratification and identification of new genes involved in structural and sequence variations in near haploid lymphoblastic leukemia. Genes Chromosomes Cancer 52, 564–579.

Chun, P., 2015. Histone deacetylase inhibitors in hematological malignancies and solid tumors. Arch. Pharmacal Res. 38, 933–949.

Coiffier, B., Thieblemont, C., Van Den Neste, E., Lepeu, G., Plantier, I., Castaigne, S., Lefort, S., Marit, G., Macro, M., Sebban, C., Belhadj, K., Bordessoule, D., Ferme, C., Tilly, H., 2010. Long-term outcome of patients in the LNH-98.5 trial, the first randomized study comparing rituximab-CHOP to standard CHOP chemotherapy in DLBCL patients: a study by the Groupe d'Etudes des Lymphomes de l'Adulte. Blood 116, 2040–2045.

Cong, L., Ran, F.A., Cox, D., Lin, S., Barretto, R., Habib, N., Hsu, P.D., Wu, X., Jiang, W., Marraffini, L.A., Zhang, F., 2013. Multiplex genome engineering using CRISPR/Cas systems. Science 339, 819–823.

Cox, J., Mann, M., 2008. MaxQuant enables high peptide identification rates, individualized p.p.b.-range mass accuracies and proteome-wide protein quantification. Nat. Biotechnol. 26, 1367–1372.

Dave, S.S., Fu, K., Wright, G.W., Lam, L.T., Kluin, P., Boerma, E.J., Greiner, T.C., Weisenburger, D.D., Rosenwald, A., Ott, G., Muller-Hermelink, H.K., Gascoyne, R.D., Delabie, J., Rimsza, L.M., Braziel, R.M., Grogan, T.M., Campo, E., Jaffe, E.S., Dave, B.J., Sanger, W., Bast, M., Vose, J.M., Armitage, J.O., Connors, J.M., Smeland, E.B., Kvaloy, S., Holte, H., Fisher, R.I., Miller, T.P., Montserrat, E., Wilson, W.H., Bahl, M., Zhao, H., Yang, L., Powell, J., Simon, R., Chan, W.C., Staudt, L.M., Lymphoma/Leukemia Molecular Profiling, P, 2006. Molecular diagnosis of Burkitt's lymphoma. N. Engl. J. Med. 354, 2431–2442.

Dimitrova, L., Seitz, V., Hecht, J., Lenze, D., Hansen, P., Szczepanowski, M., Ma, L., Oker, E., Sommerfeld, A., Jundt, F., Klapper, W., Hummel, M., 2014. PAX5 overexpression is not enough to reestablish the mature B-cell phenotype in classical Hodgkin lymphoma. Leukemia 28, 213–216.

Fantin, V.R., Loboda, A., Paweletz, C.P., Hendrickson, R.C., Pierce, J.W., Roth, J.A., Li, L., Gooden, F., Korenchuk, S., Hou, X.S., Harrington, E.A., Randolph, S., Reilly, J.F., Ware, C.M., Kadin, M.E., Frankel, S.R., Richon, V.M., 2008. Constitutive activation of signal transducers and activators of transcription predicts vorinostat resistance in cutaneous T-cell lymphoma. Cancer Res. 68, 3785–3794.

Fischer, J.J., Dalhoff, C., Schrey, A.K., Graebner, O.Y., Michaelis, S., Andrich, K., Glinski, M., Kroll, F., Sefkow, M., Dreger, M., Koester, H., 2011a. Dasatinib, imatinib and staurosporine capture compounds – complementary tools for the profiling of kinases by Capture Compound Mass Spectrometry (CCMS). J. Proteomics 75, 160–168.

Fischer, J.J., Michaelis, S., Schrey, A.K., Diehl, A., Graebner, O.Y., Ungewiss, J., Horzowski, S., Glinski, M., Kroll, F., Dreger, M., Koester, H., 2011b. SAHA Capture Compound–a novel tool for the profiling of histone deacetylases and the identification of additional vorinostat binders. Proteomics 11, 4096–4104.

Fiskus, W., Rao, R., Fernandez, P., Herger, B., Yang, Y., Chen, J., Kolhe, R., Mandawat, A., Wang, Y., Joshi, R., Eaton, K., Lee, P., Atadja, P., Peiper, S., Bhalla, K., 2008. Molecular and biologic characterization and drug sensitivity of pan-histone deacetylase inhibitor-resistant acute myeloid leukemia cells. Blood 112, 2896–2905.

Flicek, P., Amode, M.R., Barrell, D., Beal, K., Billis, K., Brent, S., Carvalho-Silva, D., Clapham, P., Coates, G., Fitzgerald, S., Gil, L., Giron, C.G., Gordon, L., Hourlier, T., Hunt, S., Johnson, N., Juettemann, T., Kahari, A.K., Keenan, S., Kulesha, E., Martin, F.J., Maurel, T., McLaren, W.M., Murphy, D.N., Nag, R., Overduin, B., Pignatelli, M., Pritchard, B., Pritchard, E., Riat, H.S., Ruffier, M., Sheppard, D., Taylor, K., Thormann, A., Trevanion, S.J., Vullo, A., Wilder, S.P., Wilson, M., Zadissa, A., Aken, B.L., Birney, E., Cunningham, F., Harrow, J., Herrero, J., Hubbard, T.J., Kinsella, R., Muffato, M., Parker, A., Spudich, G., Yates, A., Zerbino, D.R., Searle, S.M., 2014. Ensembl 2014. Nucleic Acids Res. 42, D749–D755.

Forbes, S.A., Beare, D., Gunasekaran, P., Leung, K., Bindal, N., Boutselakis, H., Ding, M., Bamford, S., Cole, C., Ward, S., Kok, C.Y., Jia, M., De, T., Teague, J.W., Stratton, M.R., McDermott, U., Campbell, P.J., 2015. COSMIC: exploring the world's knowledge of somatic mutations in human cancer. Nucleic Acids Res. 43, D805–D811.

Franceschini, A., Szklarczyk, D., Frankild, S., Kuhn, M., Simonovic, M., Roth, A., Lin, J., Minguez, P., Bork, P., von Mering, C., Jensen, L.J., 2013. STRING v9.1: protein-protein interaction networks, with increased coverage and integration. Nucleic Acids Res. 41, D808–D815.

Garcia-Manero, G., Yang, H., Bueso-Ramos, C., Ferrajoli, A., Cortes, J., Wierda, W.G., Faderl, S., Koller, C., Morris, G., Rosner, G., Loboda, A., Fantin, V.R., Randolph, S.S., Hardwick, J.S., Reilly, J.F., Chen, C., Ricker, J.L., Secrist, J.P., Richon, V.M., Frankel, S.R., Kantarjian, H.M., 2008. Phase 1 study of the histone deacetylase inhibitor vorinostat (suberoylanilide hydroxamic acid [SAHA]) in patients with advanced leukemias and myelodysplastic syndromes. Blood 111, 1060–1066.

Hoelzer, D., Walewski, J., Dohner, H., Viardot, A., Hiddemann, W., Spiekermann, K., Serve, H., Duhrsen, U., Huttmann, A., Thiel, E., Dengler, J., Kneba, M., Schaich, M., Schmidt-Wolf, I.G., Beck, J., Hertenstein, B., Reichle, A., Domanska-Czyz, K., Fietkau, R., Horst, H.A., Rieder, H., Schwartz, S., Burmeister, T., Gokbuget, N., German Multicenter Study Group for Adult Acute Lymphoblastic, L, 2014. Improved outcome of adult Burkitt lymphoma/leukemia with rituximab and chemotherapy: report of a large prospective multicenter trial. Blood 124, 3870–3879.

Hummel, M., Bentink, S., Berger, H., Klapper, W., Wessendorf, S., Barth, T.F., Bernd, H.W., Cogliatti, S.B., Dierlamm, J., Feller, A.C., Hansmann, M.L., Haralambieva, E., Harder, L., Hasenclever, D., Kuhn, M., Lenze, D., Lichter, P., Martin-Subero, J.I., Moller, P., Muller-Hermelink, H.K., Ott, G., Parwaresch, R.M., Pott, C., Rosenwald, A., Rosolowski, M., Schwaenen, C., Sturzenhofecker, B., Szczepanowski, M., Trautmann, H., Wacker, H.H., Spang, R., Loeffler, M., Trumper, L., Stein, H., Siebert, R., Molecular Mechanisms in Malignant Lymphomas Network Project of the Deutsche, K, 2006. A biologic definition of Burkitt's lymphoma from transcriptional and genomic profiling. N. Engl. J. Med. 354, 2419–2430.

Ierano, C., Chakraborty, A.R., Nicolae, A., Bahr, J.C., Zhan, Z., Pittaluga, S., Bates, S.E., Robey, R.W., 2013. Loss of the proteins Bak and Bax prevents apoptosis mediated by histone deacetylase inhibitors. Cell Cycle 12, 2829–2838.

Ivanov, M., Barragan, I., Ingelman-Sundberg, M., 2014. Epigenetic mechanisms of importance for drug treatment. Trends Pharmacol. Sci. 35, 384–396.

Iwamoto, M., Friedman, E.J., Sandhu, P., Agrawal, N.G., Rubin, E.H., Wagner, J.A., 2013. Clinical pharmacology profile of vorinostat, a histone deacetylase inhibitor. Cancer Chemother. Pharmacol. 72, 493–508.

Joosten, M., Seitz, V., Zimmermann, K., Sommerfeld, A., Berg, E., Lenze, D., Leser, U., Stein, H., Hummel, M., 2013. Histone acetylation and DNA demethylation of T cells result in an anaplastic large cell lymphoma-like phenotype. Haematologica 98, 247–254.

Karaman, M.W., Herrgard, S., Treiber, D.K., Gallant, P., Atteridge, C.E., Campbell, B.T., Chan, K.W., Ciceri, P., Davis, M.I., Edeen, P.T., Faraoni, R., Floyd, M., Hunt, J.P., Lockhart, D.J., Milanov, Z.V., Morrison, M.J., Pallares, G., Patel, H.K., Pritchard, S., Wodicka, L.M., Zarrinkar, P.P., 2008. A

quantitative analysis of kinase inhibitor selectivity. Nat. Biotechnol. 26, 127–132.
Khan, O., Fotheringham, S., Wood, V., Stimson, L., Zhang, C., Pezzella, F., Duvic, M., Kerr, D.J., La Thangue, N.B., 2010. HR23B is a biomarker for tumor sensitivity to HDAC inhibitor-based therapy. Proc. Natl. Acad. Sci. U S A 107, 6532–6537.
Kim, J.S., Lee, S.C., Min, H.Y., Park, K.H., Hyun, S.Y., Kwon, S.J., Choi, S.P., Kim, W.Y., Lee, H.J., Lee, H.Y., 2015. Activation of insulin-like growth factor receptor signaling mediates resistance to histone deacetylase inhibitors. Cancer Lett. 361, 197–206.
Kirschbaum, M., Frankel, P., Popplewell, L., Zain, J., Delioukina, M., Pullarkat, V., Matsuoka, D., Pulone, B., Rotter, A.J., Espinoza-Delgado, I., Nademanee, A., Forman, S.J., Gandara, D., Newman, E., 2011. Phase II study of vorinostat for treatment of relapsed or refractory indolent non-Hodgkin's lymphoma and mantle cell lymphoma. J. Clin. Oncol. 29, 1198–1203.
Koster, H., Little, D.P., Luan, P., Muller, R., Siddiqi, S.M., Marappan, S., Yip, P., 2007. Capture compound mass spectrometry: a technology for the investigation of small molecule protein interactions. Assay Drug Dev. Technol. 5, 381–390.
Lee, J.H., Choy, M.L., Ngo, L., Venta-Perez, G., Marks, P.A., 2011. Role of checkpoint kinase 1 (Chk1) in the mechanisms of resistance to histone deacetylase inhibitors. Proc. Natl. Acad. Sci. U S A 108, 19629–19634.
Mali, P., Yang, L., Esvelt, K.M., Aach, J., Guell, M., DiCarlo, J.E., Norville, J.E., Church, G.M., 2013. RNA-guided human genome engineering via Cas9. Science 339, 823–826.
Mann, B.S., Johnson, J.R., Cohen, M.H., Justice, R., Pazdur, R., 2007. FDA approval summary: vorinostat for treatment of advanced primary cutaneous T-cell lymphoma. Oncologist 12, 1247–1252.
McLaren, W., Pritchard, B., Rios, D., Chen, Y., Flicek, P., Cunningham, F., 2010. Deriving the consequences of genomic variants with the Ensembl API and SNP effect predictor. Bioinformatics 26, 2069–2070.
Morschhauser, F., Terriou, L., Coiffier, B., Bachy, E., Varga, A., Kloos, I., Lelievre, H., Sarry, A.L., Depil, S., Ribrag, V., 2015. Phase 1 study of the oral histone deacetylase inhibitor abexinostat in patients with Hodgkin lymphoma, non-Hodgkin lymphoma, or chronic lymphocytic leukaemia. Investig. New Drugs 33, 423–431.
Munster, P.N., Marchion, D., Thomas, S., Egorin, M., Minton, S., Springett, G., Lee, J.H., Simon, G., Chiappori, A., Sullivan, D., Daud, A., 2009. Phase I trial of vorinostat and doxorubicin in solid tumours: histone deacetylase 2 expression as a predictive marker. Br. J. Cancer 101, 1044–1050.
Ogura, M., Ando, K., Suzuki, T., Ishizawa, K., Oh, S.Y., Itoh, K., Yamamoto, K., Au, W.Y., Tien, H.F., Matsuno, Y., Terauchi, T., Yamamoto, K., Mori, M., Tanaka, Y., Shimamoto, T., Tobinai, K., Kim, W.S., 2014. A multicentre phase II study of vorinostat in patients with relapsed or refractory indolent B-cell non-Hodgkin lymphoma and mantle cell lymphoma. Br. J. Haematol. 165, 768–776.
Oki, Y., Buglio, D., Fanale, M., Fayad, L., Copeland, A., Romaguera, J., Kwak, L.W., Pro, B., de Castro Faria, S., Neelapu, S., Fowler, N., Hagemeister, F., Zhang, J., Zhou, S., Feng, L., Younes, A., 2013. Phase I study of panobinostat plus everolimus in patients with relapsed or refractory lymphoma. Clin. Cancer Res. 19, 6882–6890.
Dal Porto, J.M., Gauld, S.B., Merrell, K.T., Mills, D., Pugh-Bernard, A.E., Cambier, J., 2004. B cell antigen receptor signaling 101. Mol. Immunol. 41, 599–613.
Reeder, C.B., Ansell, S.M., 2011. Novel therapeutic agents for B-cell lymphoma: developing rational combinations. Blood 117, 1453–1462.
Richter, J., Schlesner, M., Hoffmann, S., Kreuz, M., Leich, E., Burkhardt, B., Rosolowski, M., Ammerpohl, O., Wagener, R., Bernhart, S.H., Lenze, D., Szczepanowski, M., Paulsen, M., Lipinski, S., Russell, R.B., Adam-Klages, S., Apic, G., Claviez, A., Hasenclever, D., Hovestadt, V., Hornig, N., Korbel, J.O., Kube, D., Langenberger, D., Lawerenz, C., Lisfeld, J., Meyer, K., Picelli, S., Pischimarov, J., Radlwimmer, B., Rausch, T., Rohde, M., Schilhabel, M., Scholtysik, R., Spang, R., Trautmann, H., Zenz, T., Borkhardt, A., Drexler, H.G., Moller, P., MacLeod, R.A., Pott, C., Schreiber, S., Trumper, L., Loeffler, M., Stadler, P.F., Lichter, P., Eils, R., Kuppers, R., Hummel, M., Klapper, W., Rosenstiel, P., Rosenwald, A., Brors, B., Siebert, R., Project, I.M.-S, 2012. Recurrent mutation of the ID3 gene in Burkitt lymphoma identified by integrated genome, exome and transcriptome sequencing. Nat. Genet. 44, 1316–1320.
Richter-Larrea, J.A., Robles, E.F., Fresquet, V., Beltran, E., Rullan, A.J., Agirre, X., Calasanz, M.J., Panizo, C., Richter, J.A., Hernandez, J.M., Roman-Gomez, J., Prosper, F., Martinez-Climent, J.A., 2010. Reversion of epigenetically mediated BIM silencing overcomes chemoresistance in Burkitt lymphoma. Blood 116, 2531–2542.
Saijo, K., Schmedt, C., Su, I.H., Karasuyama, H., Lowell, C.A., Reth, M., Adachi, T., Patke, A., Santana, A., Tarakhovsky, A., 2003. Essential role of Src-family protein tyrosine kinases in NF-kappaB activation during B cell development. Nat. Immunol. 4, 274–279.
Salisbury, C.M., Cravatt, B.F., 2007. Activity-based probes for proteomic profiling of histone deacetylase complexes. Proc. Natl. Acad. Sci. U S A 104, 1171–1176.
Scholtysik, R., Kreuz, M., Hummel, M., Rosolowski, M., Szczepanowski, M., Klapper, W., Loeffler, M., Trumper, L., Siebert, R., Kuppers, R., Molecular Mechanisms in Malignant Lymphomas Network Project of the Deutsche, K, 2015. Characterization of genomic imbalances in diffuse large B-cell lymphoma by detailed SNP-chip analysis. Int. J. Cancer 136, 1033–1042.
Schreiner, S.J., Schiavone, A.P., Smithgall, T.E., 2002. Activation of STAT3 by the Src family kinase Hck requires a functional SH3 domain. J. Biol. Chem. 277, 45680–45687.
Shannon, P., Markiel, A., Ozier, O., Baliga, N.S., Wang, J.T., Ramage, D., Amin, N., Schwikowski, B., Ideker, T., 2003. Cytoscape: a software environment for integrated models of biomolecular interaction networks. Genome Res. 13, 2498–2504.
Siegel, R.L., Miller, K.D., Jemal, A., 2015. Cancer statistics, 2015. CA Cancer J. Clin. 65, 5–29.
Smith, P.K., Krohn, R.I., Hermanson, G.T., Mallia, A.K., Gartner, F.H., Provenzano, M.D., Fujimoto, E.K., Goeke, N.M., Olson, B.J., Klenk, D.C., 1985. Measurement of protein using bicinchoninic acid. Anal. Biochem. 150, 76–85.
Straus, D.J., Hamlin, P.A., Matasar, M.J., Lia Palomba, M., Drullinsky, P.R., Zelenetz, A.D., Gerecitano, J.F., Noy, A., Hamilton, A.M., Elstrom, R., Wegner, B., Wortman, K., Cella, D., 2015. Phase I/II trial of vorinostat with rituximab, cyclophosphamide, etoposide and prednisone as palliative treatment for elderly patients with relapsed or refractory diffuse large B-cell lymphoma not eligible for autologous stem cell transplantation. Br. J. Haematol. 168, 663–670.
Sweetenham, J.W., Pearce, R., Taghipour, G., Blaise, D., Gisselbrecht, C., Goldstone, A.H., 1996. Adult Burkitt's and Burkitt-like non-Hodgkin's lymphoma–outcome for patients treated with high-dose therapy and autologous stem-cell transplantation in first remission or at relapse: results from the European Group for Blood and Marrow Transplantation. J. Clin. Oncol. 14, 2465–2472.
Swerdlow, S.H., Campo, E., Harris, N.L., Stein, H., Jaffe, E.S., Pileri, S.A., Thiele, J., Vadiman, J.W., 2008. WHO Classification

of Tumours of Haematopoietic and Lymphoid Tissues. World Health Organisation, Lyon.

Thompson, R.C., Vardinogiannis, I., Gilmore, T.D., 2013. The sensitivity of diffuse large B-cell lymphoma cell lines to histone deacetylase inhibitor-induced apoptosis is modulated by BCL-2 family protein activity. PloS One 8, e62822.

Visco, C., Li, Y., Xu-Monette, Z.Y., Miranda, R.N., Green, T.M., Li, Y., Tzankov, A., Wen, W., Liu, W.M., Kahl, B.S., d'Amore, E.S., Montes-Moreno, S., Dybkaer, K., Chiu, A., Tam, W., Orazi, A., Zu, Y., Bhagat, G., Winter, J.N., Wang, H.Y., O'Neill, S., Dunphy, C.H., Hsi, E.D., Zhao, X.F., Go, R.S., Choi, W.W., Zhou, F., Czader, M., Tong, J., Zhao, X., van Krieken, J.H., Huang, Q., Ai, W., Etzell, J., Ponzoni, M., Ferreri, A.J., Piris, M.A., Moller, M.B., Bueso-Ramos, C.E., Medeiros, L.J., Wu, L., Young, K.H., 2012. Comprehensive gene expression profiling and immunohistochemical studies support application of immunophenotypic algorithm for molecular subtype classification in diffuse large B-cell lymphoma: a report from the International DLBCL Rituximab-CHOP Consortium Program Study. Leukemia 26, 2103–2113.

Watanabe, T., Kato, H., Kobayashi, Y., Yamasaki, S., Morita-Hoshi, Y., Yokoyama, H., Morishima, Y., Ricker, J.L., Otsuki, T., Miyagi-Maesima, A., Matsuno, Y., Tobinai, K., 2010. Potential efficacy of the oral histone deacetylase inhibitor vorinostat in a phase I trial in follicular and mantle cell lymphoma. Cancer Sci. 101, 196–200.